Science Bulletin 67 (2022) 1182–1190

Contents lists available at ScienceDirect

Science Bulletin

journal homepage: www.elsevier.com/locate/scib

Article

Responses of Arctic sea ice to stratospheric ozone depletion

Jiankai Zhang [a,b], Wenshou Tian [a,*], John A. Pyle [c,d], James Keeble [c,d], Nathan Luke Abraham [c,d], Martyn P. Chipperfield [e], Fei Xie [f], Qinghua Yang [g,b], Longjiang Mu [h], Hong-Li Ren [i], Lin Wang [j], Mian Xu [a]

[a] College of Atmospheric Sciences, Lanzhou University, Lanzhou 730000, China
[b] Southern Marine Science and Engineering Guangdong Laboratory (Zhuhai), Zhuhai 519082, China
[c] Department of Chemistry, University of Cambridge, Cambridge CB2 1EW, UK
[d] National Centre for Atmospheric Science, Cambridge CB2 1EW, UK
[e] School of Earth and Environment, University of Leeds, Leeds LS2 9JT, UK
[f] College of Global Change and Earth System Science, Beijing Normal University, Beijing 100875, China
[g] School of Atmospheric Sciences, Sun Yat-sen University, Zhuhai 519082, China
[h] Pilot National Laboratory for Marine Science and Technology (Qingdao), Qingdao 266237, China
[i] State Key Laboratory of Severe Weather, Institute of Tibetan Plateau & Polar Meteorology, Chinese Academy of Meteorological Sciences, Beijing 100081, China
[j] Center for Monsoon System Research, Institute of Atmospheric Physics, Chinese Academy of Sciences, Beijing 100029, China

ARTICLE INFO

Article history:
Received 12 November 2021
Received in revised form 24 February 2022
Accepted 25 February 2022
Available online 26 March 2022

ABSTRACT

The Arctic has experienced several extreme springtime stratospheric ozone depletion events over the past four decades, particularly in 1997, 2011 and 2020. However, the impact of this stratospheric ozone depletion on the climate system remains poorly understood. Here we show that the stratospheric ozone depletion causes significant reductions in the sea ice concentration (SIC) and the sea ice thickness (SIT) over the Kara Sea, Laptev Sea and East Siberian Sea from spring to summer. This is partially caused by enhanced ice transport from Barents-Kara Sea and East Siberian Sea to the Fram Strait, which is induced by a strengthened and longer lived polar vortex associated with stratospheric ozone depletion. Additionally, cloud longwave radiation and surface albedo feedbacks enhance the melting of Arctic sea ice, particularly along the coast of the Eurasian continent. This study highlights the need for realistic representation of stratosphere-troposphere interactions in order to accurately predict Arctic sea ice loss.

1. Introduction

Atmospheric ozone results in local heating in the stratosphere and modulates the global energy balance by absorbing shortwave radiation and absorbing and emitting longwave radiation [1,2]. In addition to its direct radiative effect on the climate system, stratospheric ozone can also affect tropospheric weather and climate through complex chemical-radiative-dynamical coupling processes [3,4]. Both observations and numerical experiments have confirmed that the Antarctic ozone hole has resulted in a colder and strengthened polar vortex, which in turn has driven a positive trend in the Southern Annular Mode and has influenced Southern Hemispheric surface temperature, precipitation and the Hadley Cell in austral summer [5–7]. Other studies have shown that Arctic stratospheric ozone variations can affect regional tropospheric circulations and sea level pressure in the mid- and high latitudes over the Northern Hemisphere [8–11]. Additionally, stratospheric ozone may also exert an impact on polar sea ice. Some previous studies have suggested that the increase in Antarctic sea ice extent from 1979 to 2015 may be partly explained by atmospheric circulation changes associated with the Antarctic ozone hole [12,13], while others have reported higher Southern Ocean surface temperatures and sea ice loss associated with the Antarctic ozone hole [14–16]. Ferreira et al. [17] pointed out that these two contradicting responses of sea ice to Antarctic stratospheric ozone depletion are related to processes operating on different timescales. Enhanced surface westerlies and sea ice increase constitute the fast response, while increased Ekman drift leading to an upwelling of warm waters from below the mixed layer, and a consequent warming of the sea surface and reduction in sea ice cover around Antarctica, constitute the slow response.

In contrast to the overall increase in Antarctic sea ice extent in the 20th century, there has been a significant Arctic sea ice decline since 1979 [18]. It is widely believed that the Arctic sea ice loss is closely related to atmospheric and ocean circulation changes associated with global warming [19,20] and internal variability of the climate system [21]. However, the underlying mechanisms and their relative importance is still an area of active research [22,23]. The studies described above [12–17] have confirmed the

* Corresponding author.
E-mail address: wstian@lzu.edu.cn (W. Tian).

https://doi.org/10.1016/j.scib.2022.03.015

impacts of the Antarctic ozone hole on Antarctic sea ice variations. While ozone depletion is less pronounced in the Arctic than its Antarctic counterpart, stratospheric ozone concentrations above the Arctic reached a record low in spring 2020 [24], and similar low ozone concentrations have previously occurred in 1997 and 2011. A recent study has postulated that there may be a statistically significant enhancement in Arctic polar stratospheric cloud formation and extreme stratospheric ozone depletion in the future under high-emissions scenarios [25]. A question arises as to whether extreme Arctic stratospheric ozone depletion may significantly affect Arctic sea ice. Stone et al. [26] reported that the inclusion of stratospheric ozone can improve the forecast potential of Arctic regional sea ice, although the mechanisms linking the two remain unclear. This study addresses this question using sea ice data from both observations and a chemistry-climate model with a coupled ocean (Community Earth System Model, CESM, see details in Methods section). Our results show that extreme Arctic stratospheric ozone depletion could significantly decrease the sea ice over the Kara Sea, East Siberian Sea and Chukchi Sea, suggesting that extreme stratospheric ozone depletion may pose a threat to the Arctic cryosphere.

2. Materials and methods

2.1. Data

Gridded monthly mean sea ice concentration (SIC) data with a horizontal resolution of 25 km × 25 km for the period 1980–2020 is publicly available from the National Snow and Ice Data Center (NSIDC, https://nsidc.org/data/G02202/versions/4) [27]. Then the NSIDC SIC is interpolated to the horizontal resolution of 1° latitude by 1° longitude. Sea ice thickness (SIT) for the period 1980–2020 is obtained from the Pan-Arctic Ice Ocean Modeling and Assimilation System (PIOMAS) [28]. If climatological mean SIC is less than 10% and SIT is less than 0.15 m, i.e., these regions are ice-free, and the observed values are set as missing values to exclude these regions from the analysis.

Monthly mean temperature, wind, geopotential height and mean sea level pressure are taken from the National Aeronautics and Space Administration's Modern-Era Retrospective Analysis for Research and Applications, version 2 (MERRA2) reanalysis dataset [29]. The MERRA2 dataset covers the period 1980–2020 and has a horizontal resolution of 1.25° latitude by 1.25° longitude and a vertical resolution of 42 levels, extending from the surface to 0.1 hPa. Total column ozone during 1980–2020 is derived from the Multi Sensor Reanalysis version 2 (MSR2) dataset that assimilates data from several total ozone satellite instruments, including the Total Ozone Mapping Spectrometer (TOMS), the Solar Backscatter Ultraviolet (SBUV) instrument, and the Global Ozone Monitoring Experiment (GOME) [30].

2.2. Composite analysis

We define "ATCO index" as the linearly detrended and normalized Arctic total column ozone averaged between 60° and 90°N in March, calculated here using the MSR2 data. The criterion for low and high ozone cases used in this study is that the ATCO index is less than or greater than −1 or +1 standard deviation, respectively. Using this metric, the low ozone years are 1990, 1992, 1993, 1995, 1996, 1997, 2000, 2011 and 2020, while the high ozone years are 1980, 1989, 1999, 2010 and 2018. The composite mean in this study for a given field is calculated by the difference in the linearly detrended monthly mean field between low and high ozone cases. A bootstrap resampling test is used to calculate the statistical probability that two sample populations have meaningfully distinct averages. As an example, consider two samples, X and Y (sample size: N_1 and N_2). Data batches with sample size n_1 and n_2 ($n_1 \le N_1$, $n_2 \le N_2$) are repeatedly sampled from the original samples randomly to give 1000 resamples. Key statistics (e.g., mean and variance) of these resamples are calculated to estimate the true probability distributions. Finally, the upper and lower thresholds of the 95% confidence level are calculated as the 2.5th and 97.5th percentiles of 1000-time bootstrap resampling. The difference is considered statistically significant when zero is excluded on this confidence level [31].

2.3. Model simulations

In this study we use simulations performed with the Community Earth System Model (CESM), developed by National Center for Atmospheric Research, to explore the impacts of stratospheric ozone depletion on the Arctic sea ice. The fully coupled CESM model consists of seven sub-models: the Whole Atmosphere Community Climate Model (WACCM), the Community Land Model (CLM), the river transport model (RTM), the Parallel Ocean Program (POP), the sea-ice model (CICE), a land-ice model (CISM) and a coupler model that coordinates the time evolution of all these components and transfers information among them [32]. Here the version 1.2.2 of atmosphere-ocean-coupled CESM model with specified chemistry is used, with a horizontal resolution of 1.9° latitude by 2.5° longitude and 66 vertical levels. We performed two groups of time-slice experiments, i.e., LO3 and HO3, forced by low and high ozone conditions between 1 and 500 hPa in the Arctic region (60°–90°N) derived from the composite analysis based on MERRA2 data, respectively. Outside the Arctic region, ozone in both LO3 and HO3 runs is set to the climatological mean for the period 1980–2020. For both LO3 and HO3, 10 ensemble runs were performed, for a total of 10 pairs of simulations. Each pair starts with the same initial conditions obtained from a transient run in which atmosphere and ocean have reach equilibrium for the period 1955–2000. The pairs differ from each other in that their initial atmospheric conditions are perturbed based on 1 January 2000 in order to separate stratospheric ozone impacts from internal variability. As we mainly focus on the fast response of sea ice to stratospheric ozone depletion, each pair is run for 10 years. Thus, each group of time-slice experiments (i.e., LO3 and HO3) consists of 100 years.

To verify the results of time-slice runs, two transient runs, O3clm and O3tra were performed. O3clm is forced with the climatological Arctic stratospheric ozone, that includes the seasonal cycle, averaged for the period 1980–2020, while O3tra is forced by time-evolving ozone that follows observations from 1980 to 2020. Other forcings in O3clm and O3tra, such as greenhouse gases and aerosols, are fixed at the climatological mean from 1980 to 2020.

2.4. Potential vorticity (PV) inversion

The PV inversion method is used to analyze the impacts of PV changes in the Arctic lower stratosphere associated with stratospheric ozone depletion on tropospheric circulations. The anomalies in geostrophic streamfunction (ψ') and geostrophic height associated with specified quasi-geostrophic PV anomalies above 200 hPa in the Arctic region (60°–90°N) can be obtained through the inversion of the PV equation [33]:

$$PV' = \nabla_h^2\psi' + f_0^2\frac{\partial}{\partial p}\left(\frac{1}{\sigma}\frac{\partial\psi'}{\partial p}\right), \quad (1)$$

where f_0 is Coriolis parameter, p is pressure, σ is a horizontally invariant static stability and ∇_h^2 denotes horizontal Laplace operator. We use the following boundary conditions: $\psi' = 0$ at 20°N,

$\frac{\partial \psi'}{\partial y} = 0$ at 85°N, $\frac{\partial \psi'}{\partial p} = 0$ at 10 and 1000 hPa, and ψ' at longitude 0° uses a periodic boundary condition.

2.5. Radiative kernel method

To quantify the impact of radiative feedback on the surface temperature changes associated with stratospheric ozone depletion, we calculate the radiative feedback at the surface using the radiative kernel method [34–37]. The radiative sensitivity kernel $\frac{\partial R}{\partial X}$, where R denotes radiative flux and X can be temperature (T), water vapor (Q), or albedo (A), is precalculated by a partial perturbation method using a rapid radiative transfer model, RRTM [38]. The radiative feedback of T, Q and A is computed as $\Delta_X R = \frac{\partial R}{\partial X}\Delta X$.

Due to the cloud masking effects of temperature, water vapor, and albedo feedback, the cloud feedback is then calculated as follows:

$$\Delta_{cld}R = \Delta CRF + (K_T^0 - K_T)\Delta T + (K_Q^0 - K_Q)\Delta Q + (K_A^0 - K_A)\Delta A + (G^0 - G), \quad (2)$$

where ΔCRF is the cloud radiative forcing defined as the difference in the surface radiative fluxes between all-sky and clear-sky conditions, the K^0 and K are the clear-sky and all-sky kernels, and G^0 and G are the clear-sky and all-sky forcing. All the radiative fluxes are defined to be downward positive.

3. Results

3.1. Connection between Arctic ozone and sea ice

To assess the impacts of stratospheric ozone depletion on the Arctic sea ice, we compare the extremely low (including the 1997, 2011 and 2020 cases) and high March Arctic ozone composites (see Method section and Fig. S1 online). Fig. 1a, b shows the composite differences in observed SIC during spring and summer between low and high stratospheric ozone cases. There are negative SIC anomalies in the Kara Sea during spring in low ozone cases compared with high ozone cases, suggesting that the Kara sea ice cover in spring is reduced when Arctic stratospheric ozone is decreased. The regions with reduced SIC extend to the East Siber-

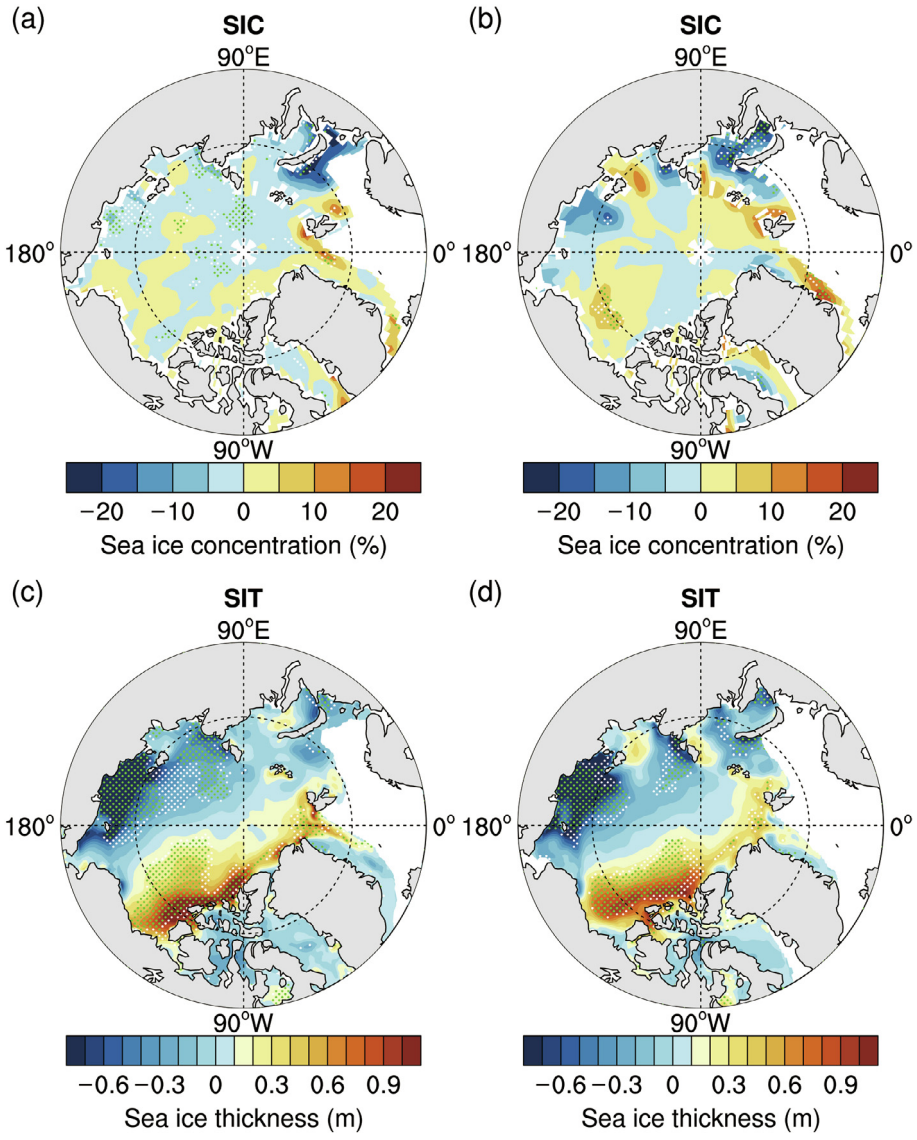

Fig. 1. Percentage differences in SIC (a, b) and differences in SIT (c, d), averaged during March–April–May (a, c) and June–July–August (b, d). The SIC data are derived from the NSIDC data, while the SIT data are derived from the PIOMAS reanalysis data between low and high ozone cases. White and green dotted regions indicate statistical significance at 90% and 95% confidence level according to a bootstrap test, respectively.

ian Sea and Chukchi Sea during summer in low ozone cases, although there are some areas with non-significant positive SIC anomalies in the Laptev Sea (Fig. 1b). SIC along the Fram Strait is increased during low ozone cases when compared with high ozone cases. Using PIOMAS reanalysis data with ocean and sea-ice observations assimilated, we can analyze the SIT changes associated with anomalous Arctic stratospheric ozone changes. Fig. 1c, d shows the composite SIT differences during spring and summer between low and high ozone cases. Note that the SIT anomalies in the Kara Sea, Laptev Sea, East Siberian Sea and Chukchi Sea during spring and summer in low ozone cases are significantly smaller than those in high ozone cases. In contrast, when Arctic stratospheric ozone is extremely low, the SIT to the north of the Canadian Arctic Archipelago is larger than normal. The significant SIT changes in the Arctic regions suggest that the extreme stratospheric ozone depletion may have impacts on both sea ice cover and volume.

Fig. S2a (online) shows the lead-lag correlation coefficients between March ATCO and SIC over the Kara Sea. Note that the positive correlation coefficient has become significant at the 99% confidence level since March (0 month) and reaches its maximum 2 months later. In addition, the correlation coefficient between ATCO and SIC is statistically significant at the 99% level from March to July (0–4 months). Fig. S2b shows the lead-lag correlation coefficients between March ATCO and SIT averaged over the Laptev Sea, East Siberian Sea and Chukchi Sea. There are significant positive correlations between ATCO and SIT throughout the spring and summer (0–5 months) and the maximum correlation coefficient occurs 1–2 months later. The abovementioned results indicate that stratospheric ozone can be a precursor signal for the sea ice changes in some Arctic regions, which agrees with the significant sea ice changes during spring and summer seen in the composite results.

The results obtained so far are based on composite analysis using observations, which can be used to highlight the link between stratospheric ozone depletion and sea ice changes but does not allow for the identification of a causal link between the two. Using the coupled ocean-ice version of the CESM model, we performed two time-slice sensitivity runs (LO3 and HO3, see Method section) forced by extremely low and high March strato-

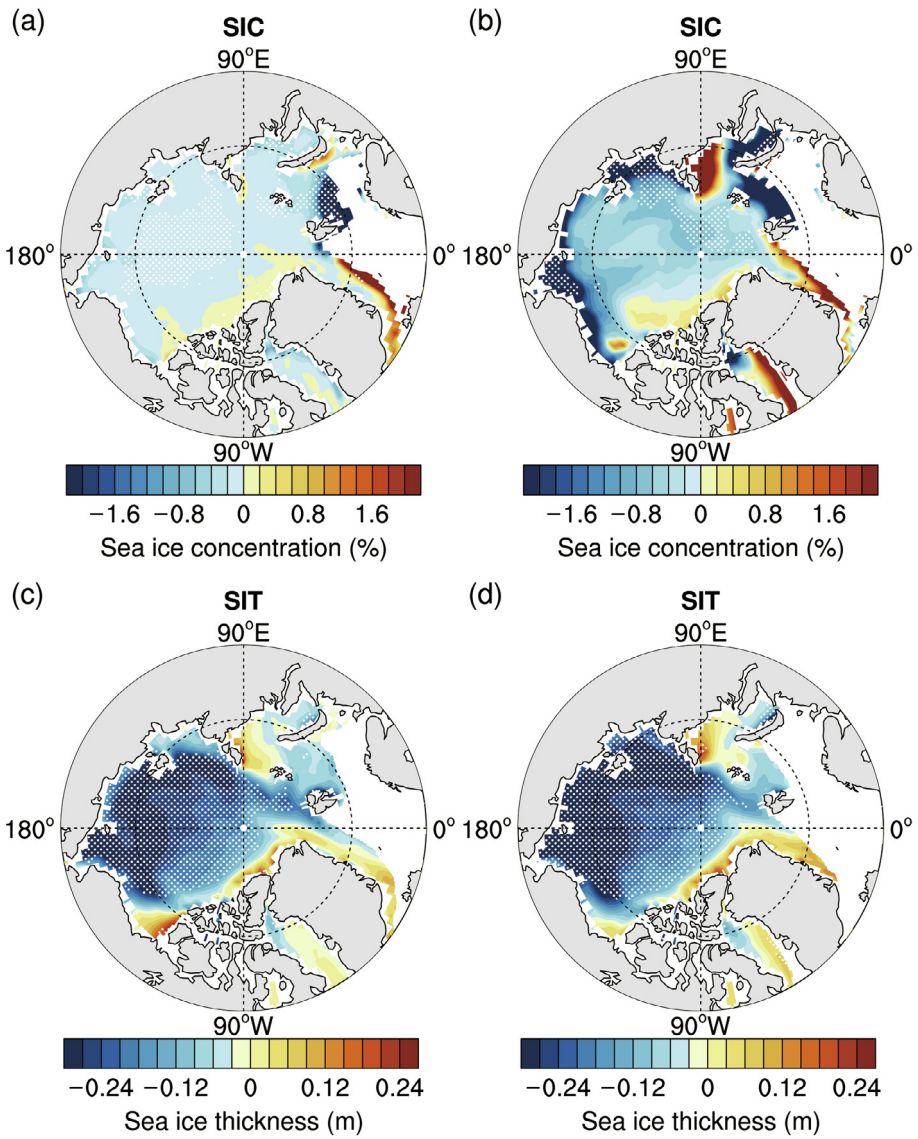

Fig. 2. Percentage differences in SIC (a, b) and differences in SIT (c, d), averaged during March–April–May (a, c) and June–July–August (b, d) between CESM LO3 and HO3. White dotted regions indicate statistical significance at 95% confidence level according to a bootstrap test.

spheric ozone conditions, respectively, to separate the stratospheric ozone impact on sea ice from internal variability. In order to make a better comparison with the composite analysis of the observational datasets discussed above, we set the same areas of open water in Fig. 2 as those in Fig. 1. Calculating differences between the LO3 and HO3 ensembles, SIC is reduced in the Kara Sea during spring and summer when Arctic ozone is low (Fig. 2a, b). The negative SIC differences in the Laptev Sea and Chukchi Sea during summer are statistically significant, whereas there are positive SIC differences along the Fram Strait between LO3 and HO3 (Fig. 2a, b), which are similar to the composite analysis. Furthermore, there is also lower SIT in the Laptev Sea, East Siberian Sea and Chukchi Sea in LO3 than those in HO3 during spring and summer (Fig. 2c, d). Although the simulated positive SIT anomalies to the north of the Canadian Arctic Archipelago are relatively weaker than those in the composite analysis of the observations (Fig. 1 c, d), the CESM model essentially supports the findings derived from observations that sea ice cover and volume in the Kara Sea, Laptev Sea, East Siberian Sea and Chukchi Sea are reduced during periods of large Arctic springtime stratospheric ozone depletion.

It should be noted that there are some discrepancies between the observation composite analysis and model simulation in the magnitudes of simulated SIC and SIT responses, particularly over the Arctic Ocean and to the north of the Canadian Arctic Archipelago. The magnitudes of SIC and SIT anomalies in the model simulations are relatively smaller than those in the composite analysis (comparing Figs. 1 and 2). These discrepancies occur because the composite analysis is not only related to stratospheric ozone depletion, but also influenced by internal variability of the climate system. In contrast, the comparison between two time-slice experiments, LO3 and HO3, separates the impacts of extreme stratospheric ozone depletion on sea ice from other climate factors.

Fig. S3 (online) shows the trends of differences in SIC (SIT) between O3tra and O3clm runs (see Method section). Note that there are negative trends in SIC difference over the Kara Sea during both spring and summer, and negative SIC trends in summer over the Chukchi Sea, suggesting that stratospheric ozone changes from 1980 to 2020 contribute to the decline in SIC over these regions. The SIT differences between O3tra and O3clm in spring and summer over the Laptev Sea, Eurasian Sea, Chukchi Sea and Arctic Ocean all show significant decline from 1980 to 2020, suggesting that stratospheric ozone depletion is partially responsible for the SIT reductions over these regions. These results agree well with the time-slice results (i.e., the differences between LO3 and HO3), further supporting the impacts of stratospheric ozone depletion on the Arctic regional sea ice loss.

3.2. Mechanisms responsible for the impacts of stratospheric ozone on sea ice

While the Arctic stratospheric ozone variability is dominated by dynamical processes, extreme ozone depletion feeds back on the dynamics of the polar vortex. Using the two large-ensemble experiments forced by low and high ozone, we can separate the feedbacks of extreme stratospheric ozone depletion on atmospheric circulations from climate variability. Fig. S4a (online) shows the differences in geopotential height between LO3 and HO3. Note that there are negative geopotential height anomalies in the lower stratosphere due to ozone-radiative cooling effects, which are significant from April to August. Fig. S4b (online) shows the position of the red/blue "zero-wind" lines from 200 to 1 hPa. Note that the zero-wind lines mainly occur in May–June for LO3, which are later than those in April–May for HO3, suggesting that there is a delay of polar vortex breakup date during low-ozone years compared with high-ozone years. This analysis indicates that stratospheric ozone depletion could lead to a stronger and longer-lived polar vortex through radiative-dynamical feedback processes, although the anomalous Arctic stratospheric ozone depletion is initially triggered by dynamical processes [39].

The strengthened and more persistent stratospheric polar vortex may influence the surface winds through stratosphere-troposphere coupling. In terms of the PV conservation theory [40,41], anomalously high PV anomaly in the lower stratosphere (Fig. 3a) could induce an anomalous cyclonic flow in the lower troposphere (Fig. 3c). Fig. S5a, b (online) shows the geopotential height anomalies in response to the positive PV anomalies above 200 hPa in the Arctic region 60°–90°N using the PV inversion method. The positive PV anomalies in the lower stratosphere could induce the negative geopotential height anomalies in the troposphere according to PV conservation. Consequently, sea level pressure in the polar regions during spring is lower during low ozone cases than during high ozone cases (Fig. 3e). In terms of geostrophic equilibrium theory, anomalous cyclonic flows at the surface occur in response to the positive lower stratospheric PV anomalies (Fig. S5c, d online). Also note that there are lower sea level pressure and anomalous cyclonic flow in the troposphere and at the surface accompanied by larger stratospheric PV in LO3 compared with those in HO3 (Fig. 3b, d, f), further confirming that the extreme stratospheric ozone depletion could significantly influence surface pressure and circulation.

It is worth noting that the significantly lower sea level pressure and anomalous cyclonic flows over the Barents Sea, Laptev Sea and East Siberian Sea associated with stratospheric ozone depletion could persist until summer (Fig. S6a online). Fig. S6b (online) shows the differences in sea ice motion vectors (red vectors) between LO3 and HO3. There is an anomalous cyclonic sea ice drift in the Arctic region when stratospheric ozone is decreased, and this cyclonic flow can last until summer, due to a longer "memory" in the ocean than in the atmosphere. The cyclonic anomaly in sea ice drift is closely related to the reduced sea level pressure and associated cyclonic wind flows at the surface during the low ozone cases (Fig. 3e, f). The ocean flow then transports sea ice away from the Kara Sea and the cyclonic oceanic drift can also reduce the size of the Beaufort Gyre, represented by the black anti-cyclonic vectors (Fig. S6b online), reducing the transport of sea ice into the Eurasian Arctic [42]. As a result, during low ozone cases, there is enhanced advection of multi-year ice away from the Eurasian coast and Beaufort Sea, reducing the sea ice over the East Siberian Sea (Figs. 1 and 2).

A question arises to whether radiative processes associated with extreme Arctic stratospheric ozone depletion may also modulate sea ice patterns. Fig. 4 shows the differences in radiative feedback of temperature, water vapor, cloud longwave radiation and surface albedo between LO3 and HO3. Note that cloud longwave feedback and albedo feedback make more important contributions to the surface radiative feedback associated with stratospheric ozone depletion than temperature and water vapor do. There are larger longwave cloud feedbacks over the Arctic region during spring and summer in LO3 than HO3, suggesting cloud feedbacks associated with stratospheric ozone depletion favor reductions in SIC and SIT. This is because stratospheric ozone depletion leads to lower temperatures (Fig. S7a, b online) and saturation vapor pressures in the troposphere, increasing relative humidity and cloud fraction (Fig. S7c, d online), consistent with the findings of Xia et al. [43–45] and Maleska et al. [46]. More clouds in the Arctic region could radiate back longwave radiation. In addition, the positive albedo feedback anomalies in LO3 compared with HO3 contribute most to the reductions in sea ice over the Laptev Sea, East Siberian Sea and Chukchi Sea during summer. This result suggests that thermal processes associated with stratospheric ozone depletion have an important effect on the sea ice loss along the coast of the Eurasian continent.

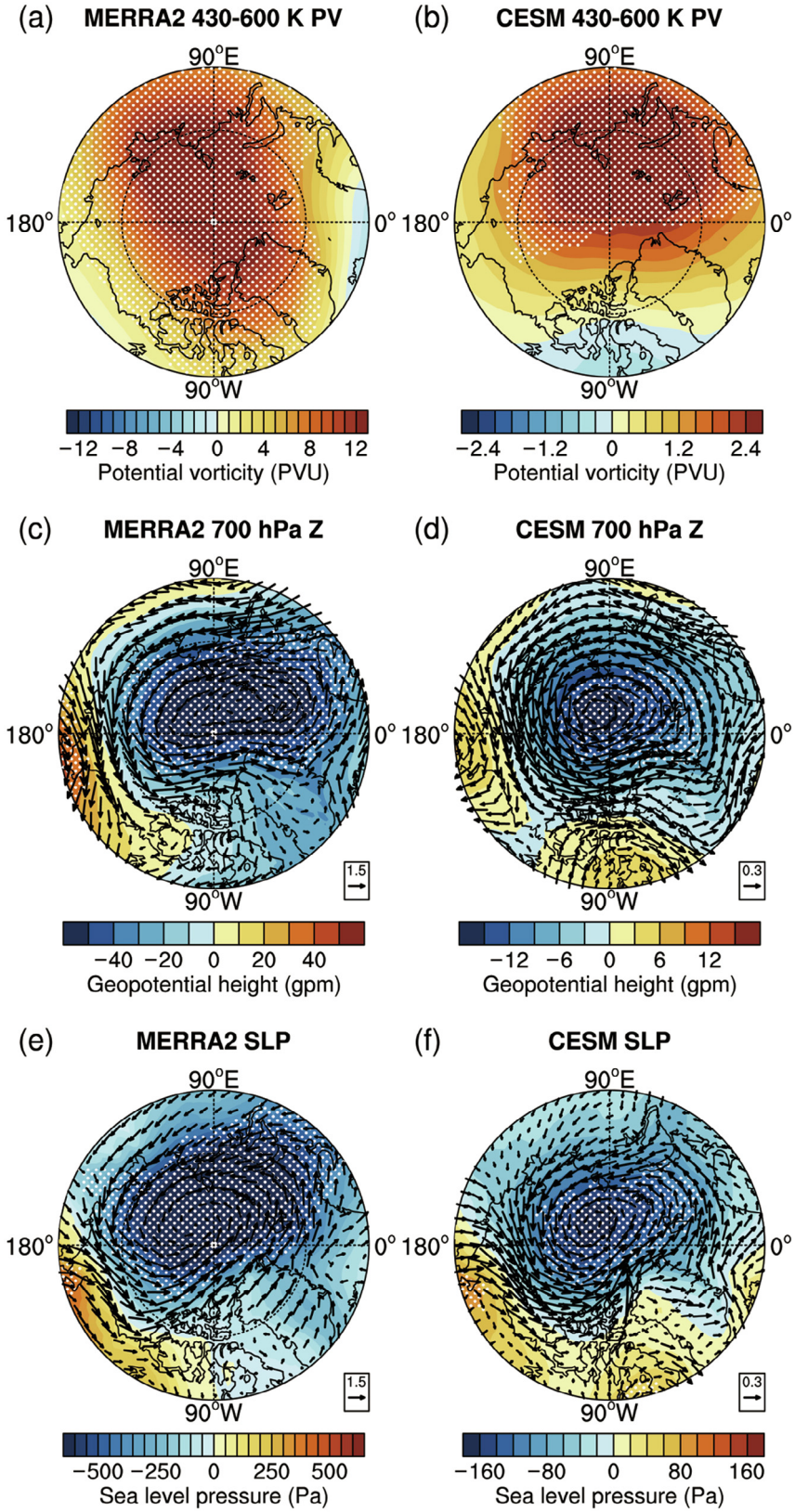

Fig. 3. Composite differences in March–April–May mean PV averaged between the isentropic layers 430–600 K (a), 700 hPa geopotential height (c) and sea level pressure (e) between low and high ozone cases derived from MERRA2 reanalysis data. Vectors in (c) and (e) represent composite differences of horizontal wind vectors at 700 and 1000 hPa, respectively. Differences in March–April–May mean PV averaged between the isentropic layers 430–600 K (b), 700 hPa geopotential height (d) and sea level pressure (f) between CESM LO3 and HO3. Vectors in (d) and (f) represent the LO3 and HO3 differences of horizontal wind vectors at 700 and 1000 hPa, respectively. White dotted regions indicate statistical significance at 95% confidence level according to a bootstrap test. The vector units are shown in the bottom right of panel (c–f).

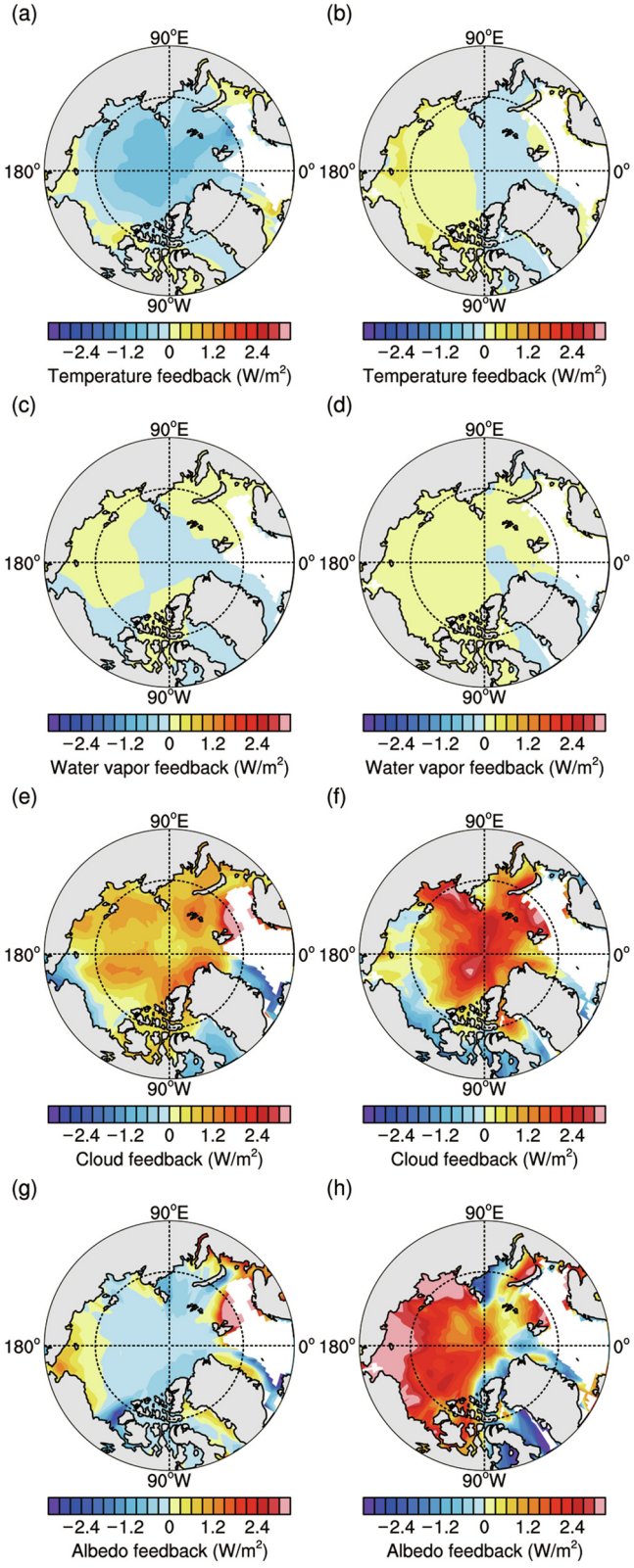

Fig. 4. Differences in temperature feedback (a, b), water vapor feedback (c, d), longwave cloud feedback (e, f), and albedo feedback (g, h) between LO3 and HO3 averaged during March–April–May (a, c, e, g) and June–July–August (b, d, f, h).

4. Discussion and conclusion

In summary, our analysis indicates springtime SIC in the Kara Sea is reduced in response to March Arctic stratospheric ozone depletion, and the region with lower SIC anomalies can extend to the East Siberian Sea in summer (Fig. 1). This feature is verified by the comparison between two time-slice runs with low and high stratospheric ozone forcings and transient runs with and without observed ozone trends (Fig. 2a, b and Fig. S3 online). In addition to the changes in sea ice cover associated with stratospheric ozone depletion, sea ice volume in the Arctic region also shows significant changes associated with stratospheric ozone variability. SIT in the Laptev Sea, East Siberian Sea and Chukchi Sea is reduced throughout the spring and summer during low ozone cases when compared with high ozone cases (Figs. 1c, d and 2c, d). Comparing LO3 and HO3, we estimate a 20% reduction of Arctic total column ozone in March may reduce SIT over the Laptev Sea and East Siberian Sea by more than 8% in summer.

We further proposed that the impacts of springtime stratospheric ozone depletion on the Arctic sea ice are achieved through dynamical and radiative coupling processes. Arctic stratospheric ozone depletion cools and strengthens the stratospheric polar vortex (Fig. S4a online), leading to a delay in breakup of the polar vortex (Fig. S4b online). Through PV conservation, there is an anomalous cyclonic flow at the surface (Fig. S5 online), enhancing sea ice drift from the Barents-Kara Sea to the East Siberian Sea and finally out through the Fram Strait (Fig. 3e, f and Fig. S6 online), reducing the sea ice cover and volume in the East Siberian Sea (Figs. 1 and 2). Additionally, Arctic stratospheric ozone depletion could increase the Arctic cloud fraction (Fig. S7 online) and radiate back more thermal radiation to the surface over the Kara Sea and East Siberian Sea (Fig. 4e, f). Positive surface albedo feedbacks in the Kara Sea and East Siberian Sea (Fig. 4g, h) are favorable for the melting of sea ice in these two regions, particularly in summer. It should be noted that our results are verified by only one climate model. Accurate quantification for the relative contribution of dynamical and radiative processes to the impacts of Arctic stratospheric ozone deletion on sea ice requires multiple model assessment.

Our results indicate that extreme Arctic stratospheric ozone depletion could significantly modulate Arctic sea ice patterns. Rex et al. [47] found that the Arctic stratospheric ozone loss during winter and early spring is closely linked to polar stratospheric cloud volume. von der Gathen et al. [25] show that local maxima of polar stratospheric cloud formation potential may rise due to stratospheric cooling in the future under high greenhouse gas emissions scenarios. Future extreme stratospheric ozone depletion events may still pose a threat to Arctic sea ice, and as a result the linkages identified in this study merit further exploration.

Conflict of interest

The authors declare that they have no conflict of interest.

Acknowledgments

This work was supported by Project of Southern Marine Science and Engineering Guangdong Laboratory (Zhuhai) (SML2021SP312), the National Natural Science Foundation of China (42075062, 42130601, and 41922044), the National Key Research & Develop-

ment Program of China (2018YFC1506003), the Fundamental Research Funds for the Central Universities, China (lzujbky-2021-ey04), and Young Doctoral Funds for Gansu Provincial Education Department (2021QB-009). We thank the scientific teams for providing National Snow and Ice Data Center (NSIDC) sea ice, Multi Sensor Reanalysis version 2 (MSR2) ozone, Pan-Arctic Ice Ocean Modeling and Assimilation System (PIOMAS) sea ice, and National Aeronautics and Space Administration's Modern-Era Retrospective Analysis for Research and Applications, version 2 (NASA–MERRA2) reanalysis data. This work was supported by Supercomputing Center of Lanzhou University.

Author contributions

Jiankai Zhang contributed to the paper writing and data analysis. Wenshou Tian proposed and conceived the study. John A. Pyle, James Keeble, Nathan Luke Abraham, Martyn P. Chipperfield and Fei Xie contributed to the discussion and paper writing. Qinghua Yang and Longjiang Mu contributed to the discussion of sea ice analysis. Hong-Li Ren, Lin Wang and Mian Xu contributed to the discussion of stratosphere-troposphere coupling. Wenshou Tian led the preparation of the manuscript with contribution from all authors.

Appendix A. Supplementary materials

Supplementary materials to this article can be found online at https://doi.org/10.1016/j.scib.2022.03.015.

References

[1] Ramaswamy V, Dickinson R. The role of stratospheric ozone in the zonal and seasonal radiative energy balance of the earth-troposphere system. J Atmos Sci 1979;36:1084–104.
[2] Forster P, Shine K. Radiative forcing and temperature trends from stratospheric ozone changes. J Geophys Res-Atmos 1997;102:10841–55.
[3] Isaksen I, Granier C, Myhre G, et al. Atmospheric composition change: climate-chemistry interactions. Atmos Environ 2009;43:5138–92.
[4] Nowack P, Abraham N, Maycock A, et al. A large ozone-circulation feedback and its implications for global warming assessments. Nat Clim Chang 2015;5:41–5.
[5] Son S, Polvani L, Waugh D, et al. The impact of stratospheric ozone recovery on the Southern Hemisphere westerly jet. Science 2008;320:1486–9.
[6] Polvani L, Waugh D, Correa G, et al. Stratospheric ozone depletion: the main driver of twentieth-century atmospheric circulation changes in the Southern Hemisphere. J Clim 2011;24:795–812.
[7] Kang S, Polvani L, Fyfe J, et al. Impact of polar ozone depletion on subtropical precipitation. Science 2011;332:951–4.
[8] Karpechko A, Perlwitz J, Manzini E. A model study of tropospheric impacts of the Arctic ozone depletion 2011. J Geophys Res-Atmos 2014;119:7999–8014.
[9] Smith K, Polvani L. The surface impacts of Arctic stratospheric ozone anomalies. Environ Res Lett 2014;9:074015.
[10] Calvo N, Polvani L, Solomon S. On the surface impact of Arctic stratospheric ozone extremes. Environ Res Lett 2015;10:094003.
[11] Ivy D, Solomon S, Calvo N, et al. Observed connections of Arctic stratospheric ozone extremes to Northern Hemisphere surface climate. Environ Res Lett 2017;12:024004.
[12] Hall A, Visbeck M. Synchronous variability in the southern hemisphere atmosphere, sea ice, and ocean resulting from the annular mode. J Clim 2002;15:3043–57.
[13] Turner J, Comiso J, Marshall G, et al. Non-annular atmospheric circulation change induced by stratospheric ozone depletion and its role in the recent increase of Antarctic sea ice extent. Geophys Res Lett 2009;36:L08502.
[14] Sigmond M, Fyfe J. Has the ozone hole contributed to increased Antarctic sea ice extent? Geophys Res Lett 2010;37:L18502.
[15] Bitz C, Polvani L. Antarctic climate response to stratospheric ozone depletion in a fine resolution ocean climate mode. Geophys Res Lett 2012;39:L20705.
[16] Xia Y, Hu Y, Liu J, et al. Stratospheric ozone-induced cloud radiative effects on Antarctic sea ice. Adv Atmos Sci 2020;37:505–14.
[17] Ferreira D, Marshall J, Bitz C, et al. Antarctic ocean and sea ice response to ozone depletion: a two-time-scale problem. J Clim 2015;28:1206–26.
[18] Intergovernmental Panel on Climate Change (IPCC). Climate change 2014: synthesis report. In: Contribution of Working Groups I, II and III to the Fifth Assessment Report of the Intergovernmental Panel on Climate Change. Geneva: IPCC; 2014.
[19] Screen J, Simmonds I. The central role of diminishing sea ice in recent Arctic temperature amplification. Nature 2010;464:1334–7.
[20] Ding Q, Schweiger A, L'Heureux M, et al. Influence of high-latitude atmospheric circulation changes on summertime Arctic sea ice. Nat Clim Chang 2017;7:289–95.
[21] Kay J, Holland M, Jahn A. Inter-annual to multi-decadal Arctic sea ice extent trends in a warming world. Geophys Res Lett 2011;38:L15708.
[22] Stroeve J, Holland M, Meier W, et al. Arctic sea ice decline: faster than forecast. Geophys Res Lett 2007;34:L09501.
[23] Winton M. Do climate models underestimate the sensitivity of Northern Hemisphere sea ice cover? J Clim 2011;24:3924–34.
[24] Manney GL, Livesey NJ, Santee ML, et al. Record-low Arctic stratospheric ozone in 2020: MLS observations of chemical processes and comparisons with previous extreme winters. Geophys Res Lett 2020;47:e2020GL089063.
[25] von der Gathen P, Kivi R, Wohltmann I, et al. Climate change favours large seasonal loss of Arctic ozone. Nat Commun 2021;12:3886.
[26] Stone KA, Solomon S, Kinnison DE. Prediction of Northern Hemisphere regional sea ice extent and snow depth using stratospheric ozone information. J Geophys Res 2020;125. e2019JD031770.
[27] Meier WN, Fetterer F, Windnagel AK, et al. NOAA/NSIDC climate data record of passive microwave sea ice concentration, version 4. Boulder: National Snow and Ice Data Center; 2021.
[28] Zhang J, Rothrock D. Modeling global sea ice with a thickness and enthalpy distribution model in generalized curvilinear coordinates. Mon Weather Rev 2003;131:845–61.
[29] Gelaro R, McCarty W, Suárez M. The modern-era retrospective analysis for research and applications, version 2 (MERRA-2). J Clim 2017;30:5419–54.
[30] Van der AR, Allaart M, Eskes H. Extended and refined multi sensor reanalysis of total ozone for the period 1970–2012. Atmos Meas Tech 2015;8:3021–35.
[31] Wilks D. Statistical methods in the atmospheric sciences. Amsterdam: Elsevier; 1995. p. 467.
[32] Marsh DR, Mills MJ, Kinnison DE, et al. Climate change from 1850 to 2005 simulated in CESM1 (WACCM). J Clim 2013;26:7372–91.
[33] Hartley DE, Villarin JT, Black RX, et al. A new perspective on the dynamical link between the stratosphere and troposphere. Nature 1998;391:471–4.
[34] Soden BJ, Held IM, Colman R, et al. Quantifying climate feedbacks using radiative kernels. J Clim 2008;21:3504–20.
[35] Shell KM, Kiehl JT, Shields CA. Using the radiative kernel technique to calculate climate feedbacks in NCAR's Community Atmospheric Model. J Clim 2008;21:2269–82.
[36] Huang Y, Xia Y, Tan X. On the pattern of CO_2 radiative forcing and poleward energy transport. J Geophys Res 2017;122:10578–510593.
[37] Huang Y, Chou G, Xie Y, et al. Radiative control of the interannual variability of Arctic sea ice. Geophys Res Lett 2019;46:9899–908.
[38] Mlawer EJ, Taubman SJ, Brown PD, et al. Radiative transfer for inhomogeneous atmospheres: RRTM, a validated correlated-k model for the longwave. J Geophys Res 1997;102:16663–82.
[39] Feng W, Dhomse SS, Arosio C, et al. Arctic ozone depletion in 2019/20: roles of chemistry, dynamics and the Montreal Protocol. Geophys Res Lett 2021;48. e2020GL091911.
[40] Hoskins BJ, McIntyre ME, Robertson AW. On the use and significance of isentropic potential vorticity maps. Q J R Meteorol Soc 1985;111:877–946.
[41] Ambaum M, Hoskins B. The NAO troposphere–stratosphere connection. J Clim 2002;15:1969–78.
[42] Smith K, Polvani L, Tremblay L. The impact of stratospheric circulation extremes on minimum Arctic sea ice extent. J Clim 2018;31:7169–83.
[43] Xia Y, Hu Y, Huang Y. Strong modification of stratospheric ozone forcing by cloud and sea-ice adjustments. Atmos Chem Phys 2016;16:1–20.
[44] Xia Y, Hu Y, Huang Y, et al. Stratospheric ozone loss-induced cloud effects lead to less surface ultraviolet radiation over the Siberian Arctic in spring. Environ Res Lett 2021;16:084057.
[45] Xia Y, Hu Y, Huang Y, et al. Significant contribution of severe ozone loss to the Siberian-Arctic surface warming in spring 2020. Geophys Res Lett 2021;48. e2021GL092509.
[46] Maleska S, Smith K, Virgin J. Impacts of stratospheric ozone extremes on Arctic high cloud. J Clim 2020;33:8869–84.
[47] Rex M, Salawitch R, von der Gathen P, et al. Arctic ozone loss and climate change. Geophys Res Lett 2004;31:L04116.

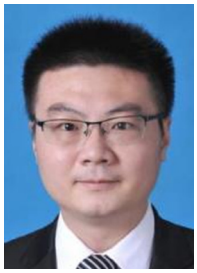

Jiankai Zhang is a professor of College of Atmospheric Sciences at Lanzhou University. His research interest includes stratosphere-troposphere coupling and impacts of Arctic climate change on midlatitude weather and climate.

Wenshou Tian is a professor of College of Atmospheric Sciences at Lanzhou University. His research interest includes stratosphere-troposphere coupling and interactions between atmospheric chemistry and climate change.